On the Mathematical Description and Simulation of Turbulent Flow in a Porous Medium Formed by an Array of Elliptic Rods

Marcos H. J. Pedras
Instituto de Pesquisa e Desenvolvimento IP&D,
UNIVAP,
12244-000, São José dos Campos, SP, Brazil

Marcelo J. S. de Lemos
Mem. ASME,
Departamento de Energia - IEME,
Instituto Tecnológico de Aeronáutica - ITA,
12228-900, São José dos Campos, SP, Brazil
e-mail: delemos@mec.ita.br

Many engineering and environmental system analyses can benefit from appropriate modeling of turbulent flow in porous media. Through the volumetric averaging of the microscopic transport equations for the turbulent kinetic energy, k, and its dissipation rate, ε, a macroscopic model was proposed for such media (IJHMT, 44(6), 1081-1093, 2001). In that initial work, the medium was simulated as an infinite array of cylindrical rods. As an outcome of the volume averaging process, additional terms appeared in the equations for k and ε. These terms were here adjusted assuming now the porous structure to be modeled as an array of elliptic rods instead. Such an adjustment was obtained by numerically solving the microscopic flow governing equations, using a low Reynolds formulation, in the periodic cell composing the medium. Different porosity and Reynolds numbers were investigated. The fine turbulence structure of the flow was computed and integral parameters were presented. The adjusted model constant was compared to similar results for square and cylindrical rods. It is expected that the contribution herein provide some insight to modelers devoted to the analysis of engineering and a environmental systems characterized by a porous structure saturated by a fluid flowing in turbulent regime.
[DOI: 10.1115/1.1413244]

Keywords: Turbulence Modeling, Porous Media, Volume-average, Saturated Flow

Introduction

A number of natural and engineering systems can be characterized by some sort of porous structure through which a working fluid permeates. Turbulent boundary layer over tropical forests and spreading of chemical contaminants through underground water reservoirs are examples of important environmental flows which can benefit form appropriate mathematical treatment. Also, fluidized bed combustors and chemical catalytic reactors are subjected to pressure loss variation due to changes in the flow regime inside the pores. In petroleum extraction, the flow accelerates toward the pumping well while crossing regions of variable porosity. Turbulent regime eventually occurs, affecting overall pressure drop and well performance. In all cases, better understanding of turbulence through adequate modeling can more realistically simulate real-world environmental and engineering flows.

Classical theory when the pore Reynolds number Re_p is less than about 150 is based on the concept of a Representative Elementary Volume - REV (Darcy [1], Forchheimer [2], Brinkman [3], Ward [4], Whitaker [5], Bear [6], Vafai and Tien [7], Whitaker [8]. For high Reynolds number ($Re_p > 300$), turbulence occurs within the pores (Prausnitz and Wilhelm [9], Mickley et al. [10] and, as such, a turbulence model is necessary in order to close the mathematical problem. For that purpose, models following the *space-time* integration sequence (Lee and Howell [11], Wang and Takle [12], Antohe and Lage [13], Getachew et al. [14], and *time-space* averaging of governing equations (Masuoka and Takatsu [15], Kuwahara et al. [16], Kuwahara and Nakayama [17], Takatsu and Masuoka [18], Nakayama and Kuwahara, [19]) have been proposed. Also suggested are morphology-oriented models which follow the *time-space* sequence and are based on the Volume Average Theory (Travkin and Catton [20], Travkin et al. [21], Gratton et al. [22], Travkin and Catton [23], Travkin and Catton [24], Travkin et al. [25]). All of these different approaches lead to different sets of governing equations and, consequently, to much debate in the literature.

Another route closer to the time-space methodology was first suggested by Pedras and de Lemos [26] prior to the proposition of the *double-decomposition* concept (Pedras and de Lemos [27–29]). This idea unveiled the connection between the space-time and time-space models. The development of this concept was a step before detailed numerical solution of the flow equations were carried out in order to establish a working version of the model (de Lemos and Pedras [30], Pedras and de Lemos [31]). Computations in a spatially periodic array of cylindrical rods using the high Re k-ε closure (Rocamora and de Lemos [32]) as well as the Low Reynolds model (Pedras and de Lemos [33,34]) were used to calibrate the introduced model constant. Heat transfer (Rocamora and de Lemos [35,36,37]) and hybrid computational domains (clear fluid-porous medium) have been also considered (de Lemos and Pedras [38]). Nonisothermal recirculating flows in channels past a porous obstacle (Rocamora and de Lemos [39,40]) and through a porous insert have been calculated (Rocamora and de Lemos [41]) using the work described in Pedras and de Lemos [31].

These two different procedures, namely *space-time* and *time-space* integration sequences, have raised interesting discussions in the literature about the proper characterization of the flow. More information on the turbulence structure under the microscopic point of view may contribute for elucidating some of the fundamental questions still pending on macroscopic modeling. One of the possibilities to gather such information is to model the topology of the porous structure and resolve the microscopic flow equation within the liquid phase. This treatment reveals the microscopic flow and was used by Kuwahara et al. [16], who adopted a spatially periodic array of square rods and by Pedras and de Lemos [34], who used cylindrical rods instead. A discus-

Contributed by the Fluids Engineering Division for publication in the JOURNAL OF FLUIDS ENGINEERING. Manuscript received by the Fluids Engineering Division January 18, 2001; revised manuscript received August 8, 2001. Associate Editor: L. Mondy.

sion on the relationship between the macroscopic and microscopic treatments is found in Pedras and de Lemos [42].

Considering available experimental work reporting the existence of turbulence in such media (Macdonald et al. [43], Kececioogl u and Jiang [44], de Lemos and Pedras [30], and Pedras and de Lemos [31], proposed a macroscopic turbulence model through the volumetric averaging of the microscopic k-ε equations. This macroscopic model, in contrast with the microscopic k-ε equations, presents two extra terms that represent extra transport/production of turbulence energy due to the presence of the solid material inside the integrated volume.

The aim of the present contribution is to adjust these new terms by numerically solving the flow field within a spatially periodic array of elliptic rods. Both low and high Re k-ε models are employed. Additional constants are determined and, with the macroscopic turbulence model so adjusted, the turbulence kinetic energy and its dissipation rate are compared with existing macroscopic flow solutions presented in the literature.

Microscopic Versus Macroscopic Turbulence

In a recent review, Lage [44], points out a distinction between *macroscopic* and *microscopic* turbulence within a porous medium. *Microscopic* turbulence was understood as the fluid regime existing within the pore whereas *macroscopic* turbulence would be the result of volume-averaging the instantaneous signal of probes distinctly located inside a REV. A more quantitative description of **macroscopic** turbulence has been proposed by Pedras and de Lemos [29], who suggested the existence of two macroscopically defined turbulence kinetic energy. The first one was formed by time-averaging the fluctuating volume-averaged velocity, $k_m = \overline{\langle \mathbf{u}' \rangle^i \cdot \langle \mathbf{u}' \rangle^i}/2$, and the second one by taking the volume integration, within the fluid phase in a REV, of the locally defined turbulence kinetic energy $k = \overline{\mathbf{u}' \cdot \mathbf{u}'}/2$. The result is then $\langle k \rangle^i = \langle \overline{\mathbf{u}' \cdot \mathbf{u}'} \rangle^i/2$. Also, a connection between k_m and $\langle k \rangle^i$ was first shown by Pedras and de Lemos [29], by means of the double-decomposition concept therein proposed.

The behavior of $\langle k \rangle^i$ as a function of porosity ϕ was numerically computed by Pedras and de Lemos [34]. In that work, the porous medium was simulated by an infinite array of circular cylinders. The compute values for $\langle k \rangle^i$ indicated that for the same Darcy velocity, or say, same volumetric mass flow rate through the bed, the overall integrated turbulence level increases with the reduction of the medium porosity (larger rod diameter). A faster fluid running through a narrower space displays steeper velocity gradients throughout the domain. Those gradients, in turn, dictate the rate at which mean flow mechanical energy is transformed into turbulence energy. Consequently, production rates of k were higher implying in higher values of $\langle k \rangle^i$ for lower porosity.

Macroscopic Equations and Numerics

Macroscopic equations for the flow turbulent kinetic energy, following both *space-time* and *time-space* integration of local instantaneous equations, have been compared in de Lemos and Pedras [46,47]. For that, their derivation will not be repeated here. There, a general classification of models presented so far in the literature was also included. Further, de Lemos and Pedras [30], and Pedras and de Lemos [31] have applied the volume-averaging operator to the microscopic k-ε equations and proposed the following macroscopic k-ε equations:

$$\begin{aligned}
\rho\left[\frac{\partial}{\partial t}(\phi\langle k\rangle^i)+\nabla\cdot(\overline{\mathbf{u}}_D\langle k\rangle^i)\right]
&=\nabla\cdot\left[\left(\mu+\frac{\mu_{t_\phi}}{\sigma_k}\right)\nabla(\phi\langle k\rangle^i)\right]\\
&\quad-\rho\langle\overline{\mathbf{u}'\mathbf{u}'}\rangle^i:\nabla\overline{\mathbf{u}}_D+c_k\rho\phi\frac{\langle k\rangle^i|\overline{\mathbf{u}}_D|}{\sqrt{K}}-\rho\phi\langle\varepsilon\rangle^i
\end{aligned}\tag{1}$$

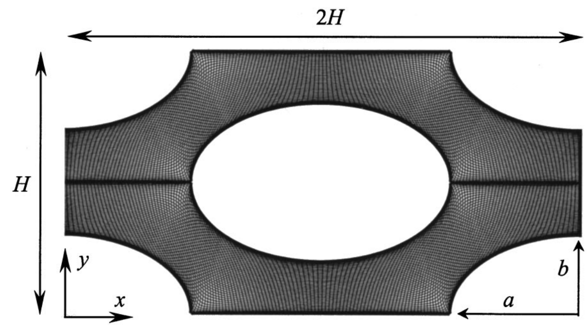

Fig. 1 Periodic cell and elliptically generated grid ($a/b=5/3$)

$$\begin{aligned}
\rho\left[\frac{\partial}{\partial t}(\phi\langle \varepsilon\rangle^i)+\nabla\cdot(\overline{\mathbf{u}}_D\langle \varepsilon\rangle^i)\right]
&=\nabla\cdot\left[\left(\mu+\frac{\mu_{t_\phi}}{\sigma_\varepsilon}\right)\nabla(\phi\langle \varepsilon\rangle^i)\right]\\
&\quad+c_{1\varepsilon}(-\rho\langle\overline{\mathbf{u}'\mathbf{u}'}\rangle^i:\nabla\overline{\mathbf{u}}_D)\frac{\langle\varepsilon\rangle^i}{\langle k\rangle^i}\\
&\quad+c_{2\varepsilon}\rho\phi\left\{c_k\frac{\langle\varepsilon\rangle^i|\overline{\mathbf{u}}_D|}{\sqrt{K}}-\frac{\langle\varepsilon\rangle^{i^2}}{\langle k\rangle^i}\right\}
\end{aligned}\tag{2}$$

with,

$$-\rho\phi\langle\overline{\mathbf{u}'\mathbf{u}'}\rangle^i=\mu_{t_\phi}2\langle\overline{\mathbf{D}}\rangle^v-\frac{2}{3}\phi\rho\langle k\rangle^i\mathbf{I}\tag{3}$$

$$\mu_{t_\phi}=\rho c_\mu\frac{\langle k\rangle^{i^2}}{\langle\varepsilon\rangle^i}\tag{4}$$

where c_k, $c_{1\varepsilon}$, $c_{2\varepsilon}$, and c_μ are nondimensional constants.

For macroscopic fully developed uni-dimensional flow in isotropic and homogeneous media, the limiting values for $\langle k \rangle^i$ and $\langle \varepsilon \rangle^i$ are given by k_ϕ and ε_ϕ, respectively. In this limiting condition, Eqs. (1) and (2) reduce to:

$$\left.\begin{aligned}
\langle\varepsilon\rangle^i=\varepsilon_\phi=c_k\frac{k_\phi|\overline{\mathbf{u}}_D|}{\sqrt{K}}\\
\frac{\langle\varepsilon\rangle^{i^2}}{\langle k\rangle^i}=c_k\frac{\varepsilon_\phi|\overline{\mathbf{u}}_D|}{\sqrt{K}}
\end{aligned}\right\}\Rightarrow\langle k\rangle^i=k_\phi\tag{5}$$

or in the following dimensionless form,

$$\frac{\varepsilon_\phi\sqrt{K}}{|\overline{\mathbf{u}}_D|^3}=c_k\frac{k_\phi}{|\overline{\mathbf{u}}_D|^2}\tag{6}$$

The coefficient c_k was adjusted in this limiting condition and for the spatially periodic cell shown in Fig. 1. This geometry represents a model for the fine porous structure. The flow was assumed to enter through the left aperture so that symmetric and periodic boundary conditions were applied. Values of k_ϕ and ε_ϕ were obtained by integrating the microscopic flow field for Reynolds number, $\mathrm{Re}_H = |\langle \overline{\mathbf{u}} \rangle^v| H/v$, from 10^4 to 10^6. The porosity, given by $\phi = 1 - ab\pi/H^2$, was varied from 0.53 to 0.85.

In the numeric model, the following microscopic transport equations were used where barred quantities represent time-averaged components and primes indicate turbulent fluctuations: Continuity equation

$$\nabla\cdot\overline{\mathbf{u}}=0\tag{7}$$

Momentum equation

$$\nabla\cdot(\rho\overline{\mathbf{u}}\overline{\mathbf{u}}) = -\nabla\overline{p} + \nabla\cdot\{\mu[\nabla\overline{\mathbf{u}} + (\nabla\overline{\mathbf{u}})^T] = \rho\overline{\mathbf{u}'\mathbf{u}'}\} \tag{8}$$

k equation

$$\nabla\cdot(\rho\overline{\mathbf{u}}k) = \nabla\cdot\left[\left(\mu + \frac{\mu_k}{\sigma_k}\right)\nabla k\right] - \rho\overline{\mathbf{u}'\mathbf{u}'}:\nabla\overline{\mathbf{u}} - \rho\varepsilon \tag{9}$$

ε equation

$$\nabla\cdot(\rho\overline{\mathbf{u}}\varepsilon) = \nabla\cdot\left[\left(\mu + \frac{\mu_t}{\sigma_\varepsilon}\right)\nabla\varepsilon\right] + [C_1(-\rho\overline{\mathbf{u}'\mathbf{u}'}:\nabla\overline{\mathbf{u}}) - C_2 f_2 \rho\varepsilon]\frac{\varepsilon}{k} \tag{10}$$

Also, the Boussinesq's concept for Reynolds stresses is given by,

$$-\rho\overline{\mathbf{u}'\mathbf{u}'} = \mu_t[\nabla\overline{\mathbf{u}} + (\nabla\overline{\mathbf{u}})^T] - \frac{2}{3}\rho k\mathbf{I} \tag{11}$$

where the turbulent viscosity is

$$\mu_t = \rho C_\mu f_\mu \frac{k}{\varepsilon} \tag{12}$$

In the above equation set σ_k, σ_ε, C_1, C_2, and C_μ are dimensionless constants whereas f_2 and f_μ are damping functions.

The use, in this work, of the low and high Re k-ε models is justified by the fact that the turbulent flow in porous media occurs for Reynolds numbers (based on the pore) relatively low. To account for the low Reynolds effects, the following damping functions were adopted (Abe et al. [48]).

$$f_2 = \left\{1 - \exp\left[-\frac{(v\varepsilon)^{0.25}n}{3.1v}\right]\right\}^2 \left\{1 - 0.3\exp\left[-\left(\frac{(k^2/v\varepsilon)}{6.5}\right)^2\right]\right\} \tag{13}$$

$$f_\mu = \left\{1 - \exp\left[-\frac{(v\varepsilon)^{0.25}n}{14v}\right]\right\}^2 \times\left\{1 + \frac{5}{(k^2/v\varepsilon)^{0.75}}\exp\left[-\left(\frac{(k^2/v\varepsilon)}{200}\right)^2\right]\right\} \tag{14}$$

where n is the coordinate normal to the wall. The model constants are given as follows,

$$C_\mu = 0.09, \quad C_1 = 1.5, \quad C_2 = 1.9, \quad \sigma_k = 1.4, \quad \sigma_\varepsilon = 1.3. \tag{15}$$

For the high Re model it was used the standard constants of Launder and Spalding [49].

With the assumption of macroscopic fully developed unidimensional flow, the following boundary conditions for the periodic cell (Fig. 1) were adopted:

$$\text{at the walls,} \quad \overline{\mathbf{u}} = 0, \quad k = 0 \quad \text{and} \quad \varepsilon = v\frac{\partial^2 k}{\partial n^2}, \tag{16}$$

on $x=0$ and $x=2H$ (periodic boundaries),

$$\overline{u}|_{x=0} = \overline{u}|_{x=2H}, \quad \overline{v}|_{x=0} = \overline{v}|_{x=2H}, \tag{17}$$

$$k|_{x=0} = k|_{x=2H}, \quad \varepsilon|_{x=0} = \varepsilon|_{x=2H}, \tag{18}$$

on $y=0$ and $y=H/2$ (symmetry planes),

$$\frac{\partial\overline{u}}{\partial y} = \frac{\partial\overline{v}}{\partial y} = \frac{\partial k}{\partial y} = \frac{\partial\varepsilon}{\partial y} = 0. \tag{19}$$

where $\overline{u}$ and $\overline{v}$ are components of $\overline{\mathbf{u}}$.

The governing equations were discretized using the finite volume procedure (Patankar [50]). The SIMPLE algorithm for the pressure-velocity coupling was adopted to correct both the pressure and the velocity fields. Process starts with the solution of the two momentum equations. Then the velocity field is adjusted in order to satisfy the continuity principle. This adjustment if obtained by solving the pressure correction equation. After that, the turbulence model equations are relaxed to update the k and ε fields. This iteration sequence is repeated until convergence is achieved. Details on the numerical discretization can be found in Rocamora and de Lemos [32] and in Pedras and de Lemos [34].

For the low Re model, the node adjacent to the wall requires that $u_\tau n/v \leq 1$. To accomplish this requirement, the grid needs a great number of points close to the wall leading to computational meshes of large sizes. In order to minimize this problem, all calculations were made in half of the periodic cell ($2H \times H/2$) and according to the boundary condition Eq. (19). The use of the symmetry boundary condition reduces the grid to 300×100 nodes.

Table 1 Summary of the integrated results

	Medium permeability	Re_H	k-ε model	$\lvert\langle\overline{\mathbf{u}}\rangle^v\rvert$	$\langle k\rangle^i$	$\langle\varepsilon\rangle^i$
$\phi=0.53$	$K=4.12\text{E-}05$	1.67E+04	low	2.51E-01	1.36E-02	1.26E-01
		1.67E+05	low	2.51E+00	1.09E+00	1.17E+02
		1.67E+05	high	2.51E+00	1.40E+00	1.21E+02
		1.67E+06	high	2.51E+01	1.62E+02	1.34E+05
$\phi=0.70$	$K=1.29\text{E-}04$	1.67E+04	low	2.51E-01	1.06E-02	5.72E-02
		1.67E+05	low	2.51E+00	8.16E-01	4.71E+01
		1.67E+05	high	2.51E+00	8.71E-01	4.45E+01
		1.67E+06	high	2.51E+01	9.99E+01	5.00E+04
$\phi=0.85$	$K=3.25\text{E-}04$	1.67E+04	low	2.51E-01	7.52E-03	2.83E-02
		1.67E+05	low	2.51E+00	5.48E-01	2.14E+01
		1.67E+05	high	2.51E+00	5.17E-01	1.79E+01
		1.67E+06	high	2.51E+01	7.52E+01	2.70E+04

(a) (b) (c)

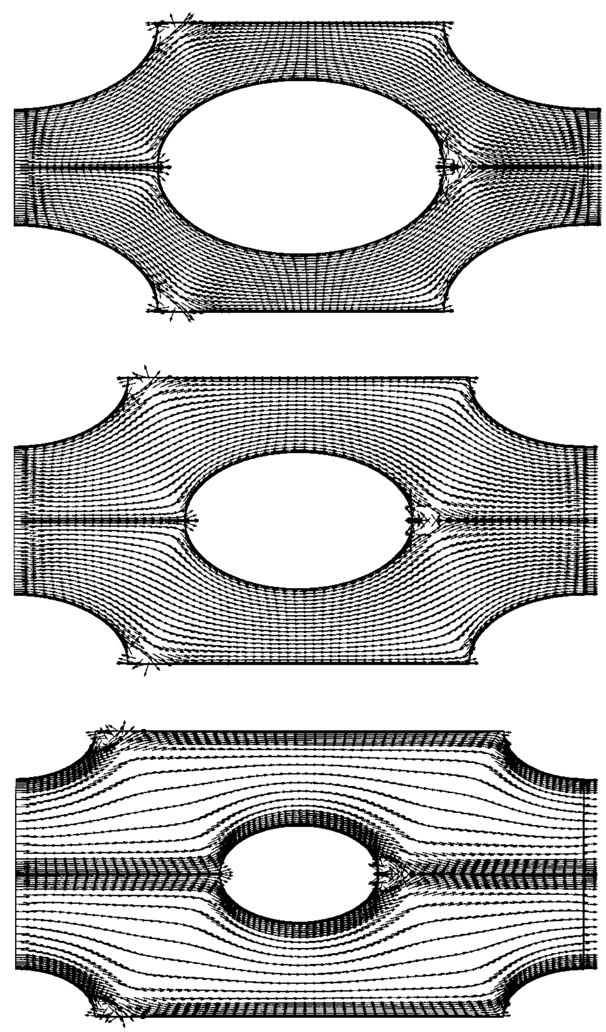

Fig. 2 Microscopic velocity field ($\mathrm{Re}_H=1.67\times10^5$): a) $\phi=0.53$, b) $\phi=0.70$ e c) $\phi=0.85$

A highly nonuniform grid arrangement was employed with concentration of nodes close to the wall. All calculations were executed using an IBM SP2 computer.

Results and Discussion

A total of eighteen runs were carried out being six for laminar flow, six with the low Re model and six using the high Re theory. Table 1 summarizes the integrated results (volumetric averaging over the periodic cell) obtained for turbulent flow (Pedras and de Lemos [51], Pedras and de Lemos [52]. The medium permeability was calculated using the procedure adopted by Kuwahara et al. [16].

Figure 2 presents velocity fields for $\mathrm{Re}_H = 1.67 \times 10^5$ (low Re model) and $\phi = 0.53$. It is observed that the flow accelerates in the upper and lower passages around the ellipse and separates at the back. As porosity decreases maintaining Re_H constant, or say, reducing the flow passage and increasing the local fluid speed, the integrated turbulence kinetic energy, $\langle k \rangle'$, increases (see Table 1). In other words, for a fixed mass flow rate through the bed, a decrease in porosity implies in accentuated velocity gradients which, in turn, result in larger production rates of k due to steep velocity gradients within the fluid. Furthermore, the increment of the fluid momentum close to the walls as porosity is reduced, for the same $|\langle \overline{\mathbf{u}} \rangle^v|$, reduces also the size of the recirculating bubble behind the elliptic rod. This effect was verified by Pedras and de Lemos [34] for an array of cylindrical rods and by Kuwahara

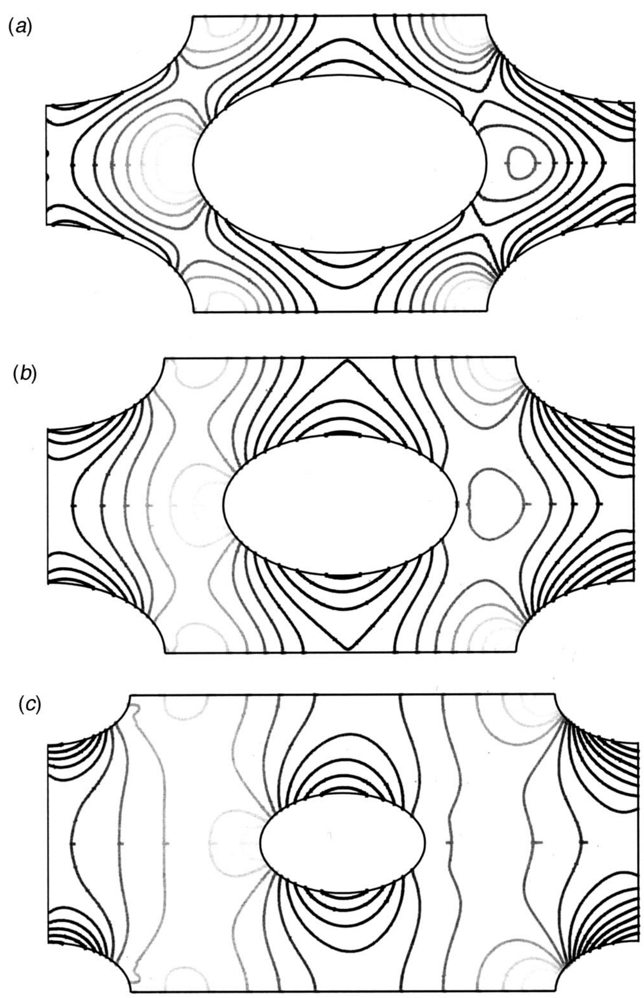

Fig. 3 Microscopic pressure field (Re_H=1.67×10^5): a) ϕ=0.53, b) ϕ=0.70 e c) ϕ=0.85

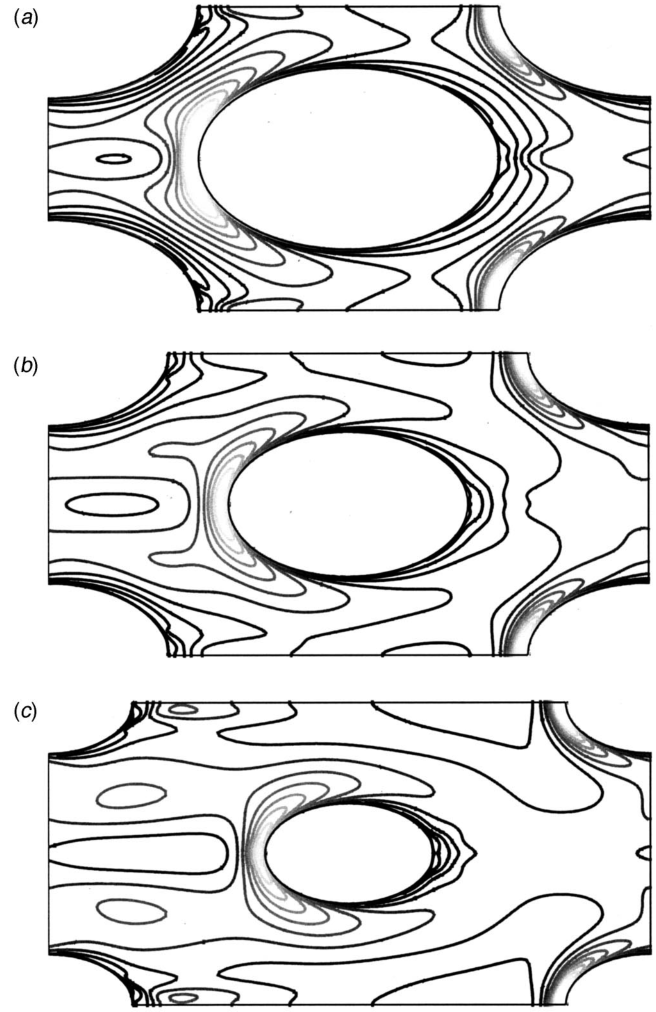

Fig. 4 Microscopic fields for k (Re_H=1.67×10^5): a) ϕ=0.53, b) ϕ=0.70 e c) ϕ=0.85

et al. [16], for an array of square cylinders. For the geometry here investigated, reduction of the wake region in Fig. 2 is more difficult to be visualized due the streamlined flow pattern around ellipses. Nevertheless, numerical values for $\langle k \rangle^i$ shown in Table 1 indicate a similar trend for $\langle k \rangle^i$ as a function of ϕ as in the other two arrangements used for comparison.

Remainder fields for pressure, k and ε, are shown in Figs. 3, 4, and 5, respectively. It is verified that the pressure increases at the front of the ellipse and decreases at the upper and lower faces. The turbulence kinetic energy is high at the front, on the top and below the bottom of the ellipse. The dissipation rate of k presents a behavior similar to the turbulence kinetic energy.

It is also interesting to point out that for the same ϕ and Re_H the integrated values shown in Table 1 for $\langle k \rangle^i$ are lower than those obtained for square (Nakayama and Kuwahara [19]) and for cylindrical rods (Pedras and de Lemos [34]). Apparently, smoother passages in between elliptic rods contributes for reducing sudden flow acceleration within the flow, reducing then overall velocity gradients and, consequently, lowering production rates $\langle k \rangle^i$.

Pressure Gradient and Constant c_k for Elliptic Rods

The macroscopic pressure gradient based on the intrinsic pressure is obtained with the help of the following equations:

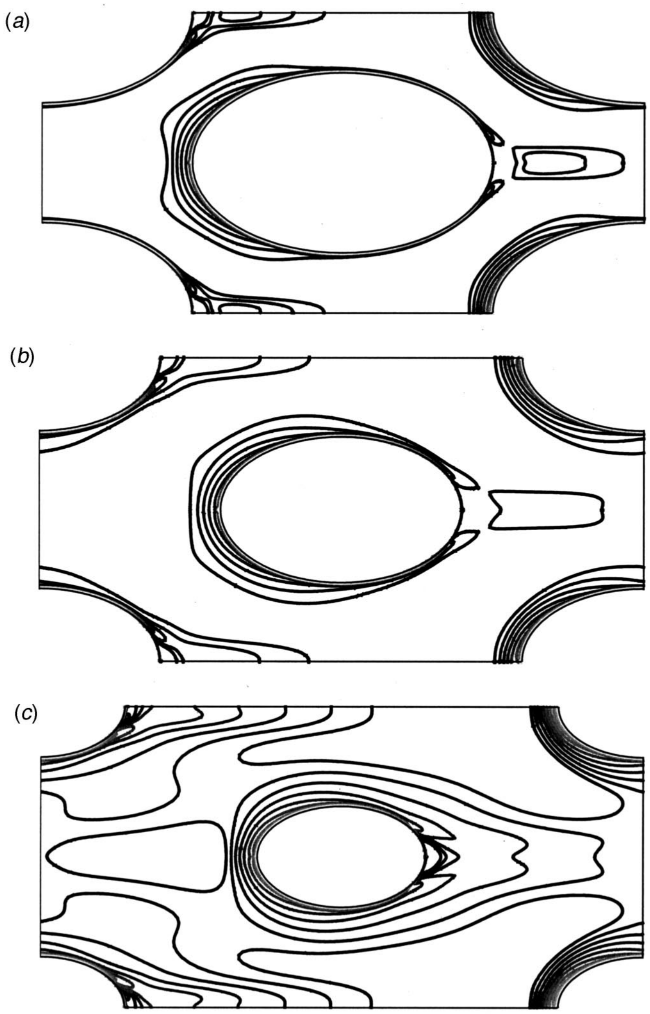

Fig. 5 Microscopic field for ε (Re_H=1.67×10^5): a) ϕ=0.53, b) ϕ=0.70 e c) ϕ=0.85

$$\frac{d\langle\overline{p}\rangle^i}{dS}=\frac{1}{2H(H/2-D/2)}\int_{D/2}^{H/2}(p|_{x=2H}-p|_{x=0})dy \qquad (20)$$

Results for the nondimensional pressure gradient versus Re_H are presented in Fig. 6, in addition to data from Kuwahara et al. [17] and Pedras and de Lemos [31], for square and cylindrical rods, respectively. Pressure gradient for elliptic rods fall lower than for square and cylindrical rods, as expected, since pressures losses over streamlined bodies are lower than those for flows where a wake region is of a larger size.

Also, for the same porosity and Reynolds number, the values for the intrinsic turbulent kinetic energy, $\langle k\rangle^i$ in Table 1 are lower than those obtained for square cylinders (Nakayama and Kuwahara [19]) and for circular rods (Pedras and de Lemos [34]). This result could be explained by recalling that, within voids formed in between the ellipses, the fluid accelerates less intensively causing lower velocity gradients and, consequently, lower production rates of k.

Once the intrinsic values of k_ϕ and ε_ϕ were obtained, they were plugged into Eq. (6). The value of c_k equal to 0.28 was found by noting the collapse of all data into the straight line shown in Fig. 7. The figure also shows data of Pedras and de Lemos [31], and Nakayama and Kuwahara [19] for cylindrical and square rods, respectively.

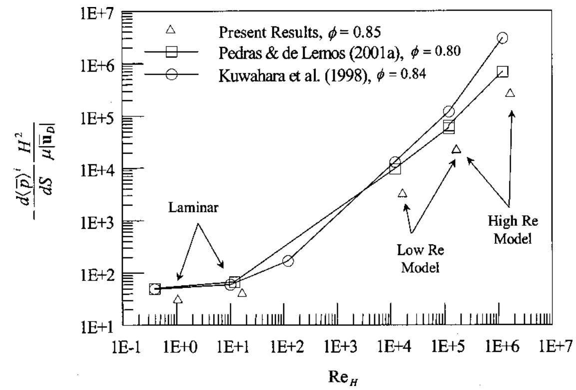

Fig. 6 Effect of Reynolds number, Re_H, on nondimensional pressure gradient

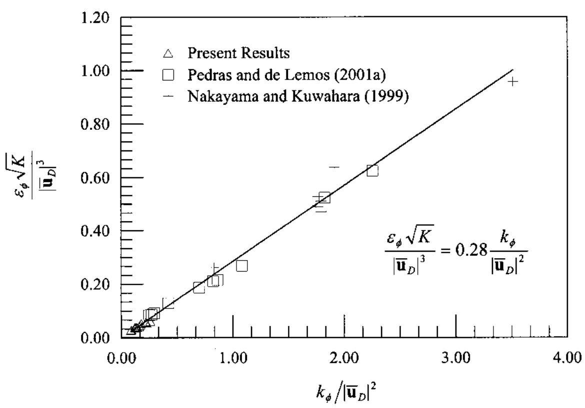

Fig. 7 Determination of value for c_k using data for different porous media, porosity and Reynolds number

Macroscopic Model Results

With the numerical evaluation of c_k, calculations using the macroscopic turbulence model above can be performed. A test case consisting in simulating the flow through a porous bed of length $10H$, starting with a preselected initial conditions greater than the final asymptotic values, is now carried out. Similar test results were reported by Pedras and de Lemos [31], and Nakayama and Kuwahara [19], being the values at entrance $\langle k\rangle^i=10k_\phi$ and $\langle\varepsilon\rangle^i=30\varepsilon_\phi$. Figures 8 and 9 show results for $\langle k\rangle^i$ and $\langle\varepsilon\rangle^i$ along the flow. Calculations are compared with similar

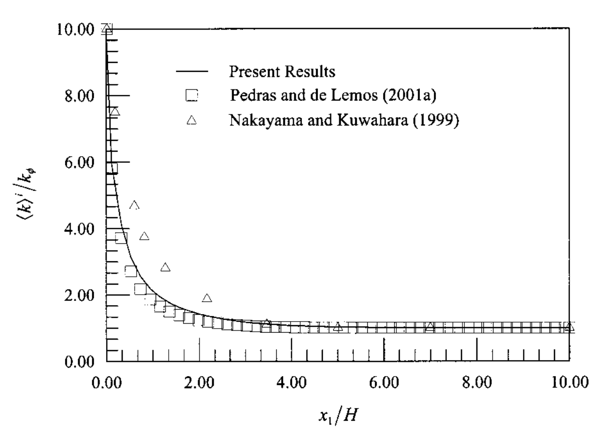

Fig. 8 Development of nondimensional turbulence kinetic energy

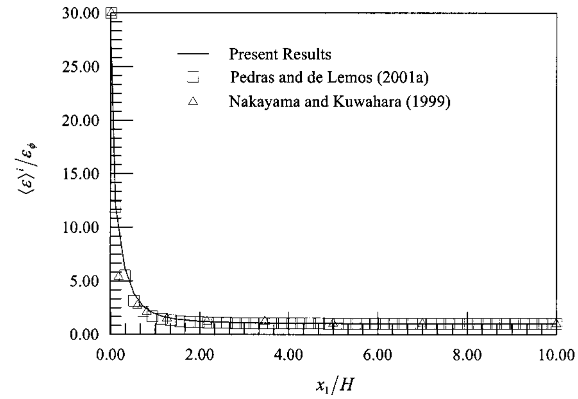

Fig. 9 Development of nondimensional dissipation rate

results of Nakayama and Kuwahara [19], for an array of square rods and with computations of Pedras and de Lemos [31] for a bed of circular cylinders. Is interesting to note that, in spite of differences on the shape of the rods, the axial decay is nearly the same in all cases indicating the coherence of the results herein with previous data published in the literature.

Concluding Remarks

This paper presented the views in the literature for characterizing turbulent flow in porous media. The equations for the flow turbulent kinetic energy were presented. A macroscopic turbulence model was adjusted for an infinite porous medium formed by spatially periodic array of elliptic rods. This adjustment was carried out by the solution of the microscopic flow field within the volume occupied by the fluid. After that, integrated flow properties were computed and the proposed model constant was determined. Then, the macroscopic model was tested comparing the numerical results of the flow in the entrance region of homogeneous isotropic porous medium with available similar results in the recent literature. Good agreement with published data was observed.

Acknowledgments

MJSdL is thankful to CNPq, Brazil, for their financial support during the course of this research.

References

[1] Darcy, H., 1856, *Les Fontaines Publiques de la Vile de Dijon*, Victor Dalmond, Paris.
[2] Forchheimer, P., 1901, ''Wasserbewegung durch Boden,'' Z. Ver. Deutsch. Ing. **45**, pp. 1782–1788.
[3] Brinkman, H. C., 1947, ''A Calculation of the Viscous Force Exerted by a Flowing Fluid on a Dense Swarm of Particles, '' Appl. Sci. Res., **A1**, pp. 27–34.
[4] Ward, J. C., 1964, ''Turbulent Flow in Porous Media,'' J. Hydraul. Div. Am. Soc. Civ. Eng. **90**, pp, 1–12.
[5] Whitaker, S., 1969, ''Advances in Theory of Fluid Motion in Porous Media,'' Ind. Eng. Chem., **61**, pp. 14–28.
[6] Bear, J., 1972, *Dynamics of Fluids in Porous Media*, American Elsevier, New York.
[7] Vafai, K., and Tien, C. L., 1981, ''Boundary and Inertia Effects on Flow and Heat Transfer in Porous Media,'' Int. J. Heat Mass Transf., **24**, pp. 195–203.
[8] Whitaker, S., 1999, *The Method of Volume Averaging*, Kluwer Academic Publishers, Dordrecht,
[9] Prausnitz, J. M., and Wilhelm, R. H., 1957, ''Turbulent Concentrations Fluctuations in a Packed Bed,'' Ind. Eng. Chem., **49**, pp. 237–246.
[10] Mickley, H. S., Smith, K. A., and Korchak, E. I., 1965, ''Fluid Flow in Packed Beds,'' Chem. Eng. Sci., **20**, pp. 237–246.
[11] Lee, K., and Howell, J. R., 1987, ''Forced Convective and Radiative Transfer Within a Highly Porous Layer Exposed to a Turbulent External Flow Field,'' *Proc. of the 1987 ASME-JSME Thermal Eng. Joint Conf.*, Vol. 2, pp. 377–386.
[12] Wang, H., and Takle, E. S., 1995, ''Boundary-Layer Flow and Turbulence Near Porous Obstacles,'' Boundary-Layer Meteorol., **74**, pp. 73–88.
[13] Antohe, B. V., and Lage, J. L., 1997, ''A General Two-Equation Macroscopic Turbulence Model for Incompressible Flow in Porous Media,'' Int. J. Heat Mass Transf., **40**, pp. 3013–3024.
[14] Getachew, D., Minkowycz, W. J., and Lage, J. L., 2000, ''A Modied Form of the k-ε Model for Turbulent Flow of an Incompressible Fluid in Porous Media,'' Int. J. Heat Mass Transf., **43**, pp. 2909–2915.
[15] Masuoka, T., and Takatsu, Y., 1996, ''Turbulence Model for Flow Through Porous Media,'' Int. J. Heat. Mass Transfer, **39**, pp. 2803–2809.
[16] Kuwahara, F., Kameyama, Y., Yamashita, S., and Nakayama, A., 1998, ''Numerical Modeling of Turbulent Flow in Porous Media Using a Spatially Periodic Array,'' J. Porous Media **1**, pp. 47–55.
[17] Kuwahara, F., and Nakayama, A., 1998, ''Numerical Modeling of Non-Darcy Convective Flow in a Porous Medium,'' *Proc. 11th Int. Heat Transf. Conf.*, Kyongyu, Korea, Aug. 23–28.
[18] Takatsu, Y., and Masuoka, T., 1998, ''Turbulent Phenomena in Flow Through Porous Media, J. Porous Media, **3**, pp. 243–251.
[19] Nakayama, A., and Kuwahara, F., 1999, ''A Macroscopic Turbulence Model for Flow in a Porous Medium,'' ASME J. Fluids Eng., **121**, pp. 427–433.
[20] Travkin, V. S., and Catton, I., 1992, ''Model of Turbulent Thermal Diffusivity and Transfer Coefficients for a Regular Packed Bed of Spheres,'' *Proc. 28th National Heat Transfer Conference*, San Diego, C-4, ASME-HTD-193, pp. 15–23.
[21] Travkin, V. S., Catton, I., and Gratton, L., 1993, ''Single-Phase Turbulent Transport in Prescribed Non-Isotropic and Stochastic Porous Media,'' *Heat Transfer in Porous Media*, ASME-HTD-240, pp. 43–48.
[22] Gratton, L., Travkin, V. S., and Catton, I., 1994, ''Numerical Solution of Turbulent Heat and Mass Transfer in a Stratified Geostatistical Porous Layer for High Permeability Media,'' ASME Proceedings HTD-vol.. 41, pp. 1–14.
[23] Travkin, V. S., and Catton, I., 1995, ''A Two Temperature Model for Turbulent Flow and Heat Transfer in a Porous Layer,'' ASME J. Fluids Eng., **117**, pp. 181–188.
[24] Travkin, V. S., and Catton, I., 1998, ''Porous Media Transport Descriptions-Non-Local, Linear and Non-Linear Against Effective Thermal/Fluid Properties,'' Adv. Colloid Interface Sci., **76-77**, pp. 389–443.
[25] Travkin, V. S., Hu, K., and Catton, I., 1999, ''Turbulent Kinetic Energy and Dissipation Rate Equation Models for Momentum Transport in Porous Media,'' *Proc. 3rd ASME/JSME Joint Fluids Engineering Conference* (on CD-ROM), Paper FEDSM99-7275, San Francisco, California, 18–23 July.
[26] Pedras, M. H. J., and de Lemos, M. J. S., 1998, ''Results for Macroscopic Turbulence Modeling for Porous Media,'' *Proc. of ENCIT98-7th Braz. Cong. Eng. Th. Sci.*, Vol. 2, pp. 1272–1277, Rio de Janeiro, Brazil, November 3-6 (in Portuguese).
[27] Pedras, M. H. J., and de Lemos, M. J. S., 1999, On Volume and Time Averaging of Transport Equations for Turbulent Flow in Porous Media, *Proc. of 3rd ASME/JSME Joint Fluids Engineering Conferernce* (on CDROM), ASME-FED-248, Paper FEDSM99-7273, ISBN 0-7918-1961-2, San Francisco, CA, July 18–25.
[28] Pedras, M. H. J., and de Lemos, M. J. S., 1999; ''Macroscopic Turbulence Modeling for Saturated Porous Media,'' *Proc. of COBEM99-15th Braz. Congr. Mech. Eng.* (on CD-ROM), ISBN: 85-85769-03-3, Águas de Lindóia, São Paulo, Brazil, November 22–26 (in Portuguese).
[29] Pedras, M. H. J., and de Lemos, M. J. S., 2000, ''On the Definition of Turbulent Kinetic Energy for Flow in Porous Media,'' Int. Commun. Heat Mass Transfer, **27**, No. 2, pp. 211–220.
[30] de Lemos, M. J. S., and Pedras, M. H. J. 2000, ''Modeling Turbulence Phenomena in Incompressible Flow Through Saturated Porous Media,'' *Proc. of 34th ASME-National Heat Transfer Conference* (on CD-ROM), ASME-HTD-I463CD, Paper NHTC2000-12120, ISBN:0-7918-1997-3, Pittsburgh, PA, August 20-22.
[31] Pedras, M. H. J., and de Lemos, M. J. S., 2001, ''Macroscopic Turbulence Modeling for Incompressible Flow Through Undeformable Porous Media,'' Int. J. Heat Mass Transf., **44**, No. 6, pp. 1081–1093.
[32] Rocamora Jr., F. D., and de Lemos, M. J. S., 1998, ''Numerical Solution of Turbulent Flow in Porous Media Using a Spatially Periodic Array and the *k*-ε Model,'' *Proc. ENCIT-98 - 7th Braz. Cong. Eng. Th. Sci.*, Vol. 2, pp. 1265–1271, Rio de Janeiro, RJ, Brazil, November 3–6.
[33] Pedras, M. H. J., and de Lemos, M. J. S., 2000, ''Numerical Solution of Turbulent Flow in Porous Media using a Spatially Periodic Cell and the Low Reynolds k-ε Model,'' *Proc. of CONEM2000 - National Mechanical Engineering Congress* (on CD-ROM), Natal, Rio Grande do Norte, Brazil, August 7–11 (in Portuguese).
[34] Pedras, M. H. J., and de Lemos, M. J. S., 2001, ''Simulation of Turbulent Flow in Porous Media Using a Spatially Periodic Array and a Low Re Two-Equation Closure,'' Numer. Heat Transfer, Part A, **39**, No. 1, pp. 35–59.
[35] Rocamora, Jr., F. D., and de Lemos, M. J. S., 1999, ''Simulation of Turbulent Heat Transfer in Porous Media Using a Spatially Periodic Cell and the k-ε Model,'' *Proc. of COBEM99 - 15th Braz. Congr. Mech. Eng.* (on CD-ROM), ISBN: 86-85769-03-3, Águas de Lindóia, São Paulo, Brazil, Nov. 22–26.
[36] Rocamora, Jr., F. D., and de Lemos, M. J. S., 2000, ''Analysis Of Convective Heat Transfer For Turbulent Flow in Saturated Porous Media,'' Int. Commun. Heat Mass Transfer, **27**, pp. 825–834.
[37] Rocamora Jr., and de Lemos, M. J. S., 2001, ''Turbulence Modeling For Non-Isothermal Flow in Undeformable Porous Media,'' *Proc. of NHTC'01, 35th National Heat Transfer Conference*, **ASME-HTD-I495CD**, Paper NHTC2001-20178, **ISBN: 0-7918-3527-8**, Anaheim, California, June 10–12.
[38] de Lemos, M. J. S., and Pedras, M. H. J., 2000, ''Simulation of Turbulent Flow Through Hybrid Porous Medium-Clear Fluid Domains,'' *Proc. of*

IMECE2000-ASME-Intern. Mech. Eng. Congr., ASME-HTD-366-5, pp. 113–122, ISBN:0-7918-1908-6, Orlando, FL, November 5–10.
[39] Rocamora, Jr., F. D., and de Lemos, M. J. S., 2000, Prediction of Velocity and Temperature Profiles for Hybrid Porous Medium-Clean Fluid Domains, ''*Proc. of CONEM2000—National Mechanical Engineering Congress* (on CD-ROM), Ntal, Rio Grande do Norte, Brazil, August 7–11.
[40] Rocamora, Jr., F. D., and de Lemos, M. J. S., 2000, ''Laminar Recirculating Flow And Heat Transfer In Hybrid Porous Medium-Clear Fluid Computational Domains,'' *Proc. of 34th ASME-National Heat Transfer Conference* (on CD-ROM), ASME-HTD-I463CD, Paper NHTC2000-12317, ISBN:0-7918-1997-3, Pittsburgh, PA, August 20–22.
[41] Rocamora, Jr., F. D., and de Lemos, M. J. S., 2000, ''Heat Transfer In Suddenly Expanded Flow in a Channel With Porous Inserts,'' *Proc. of IMECE2000 - ASME - Intern. Mech. Eng. Congr.*, ASME-HTD-366-5, pp. 191–195, ISBN:0-7918-1908-6, Orlando, FL, November 5–10.
[42] Pedras, M. H. J., and de Lemos, M. J. S., 1998, ''Analysis of Flow in Porous Media Via Volumetric Averaging of the Navier-Stokes Equations,'' Proc. of ENCIT98- 7th Braz. Cong. Eng. Th. Sci., Vol. 2, pp. 1278–1283, Rio de Janiero, Brazil, November 3–6 (in Portuguese).
[43] Macdonald, I. F., El-Sayed, M. S., Mow, K., and Dullien, F. A. L., 1979, ''Flow Through Porous Media: The Ergun Equation Revisited,'' Indust. Chem. Fundam. **18**, pp. 199–208.
[44] Kececiooglu, I., and Jiang, Y., 1994, ''Flow Through Porous Media of Packed Spheres Saturated With Water,'' ASME J. Fluids Eng., **116**, pp. 164–170.
[45] Lage, J. L., 1998, ''The Fundamental Theory of Flow Through Permeable Media From Darcy to Turbulence,'' in *Transport Phenomena in Porous Media*, D. B. Ingham and I. Pop, eds., Elsevier Science Ltd., ISBN: 0-08-042843-6, 446 pgs.
[46] de Lemos, M. J. S., and Pedras M. H. J., 2001, ''Alternative Transport Equations for Turbulent Kinetic Energy for Flow in Porous Media,'' Prof. of NHTC01, 35th Nat. Heat Transfer Conf. ASME-HTD-I49SCD Paper NHTC01-20177, ISBN: 0-7918-3527-8, Anaheim, California, June 10–12.
[47] de Lemos, M. J. S., and Pedras, M. H. J., 2001, ''Recent Mathematical Models For Turbulent Flow In Saturated Rigid Porous Media,'' ASME Journal of Fluids Engineering.
[48] Abe, K., Nagano, and Y., Kondoh, T., 1992, ''An Improved k-ε Model for Prediction of Turbulent Flows With Separation and Reattachment,'' Trans. Jpn. Soc. Mech. Eng., Ser. B, **58**, pp. 3003–3010.
[49] Launder, B. E., and Spalding, D. B., 1974, ''The Numerical Computation of Turbulent Flows,'' Comput. Methods Appl. Mech. Eng., **3**, pp. 269–289.
[50] Patankar, S. V., 1980, *Numerical Heat Transfer And Fluid Flow*, Hemisphere, New York.
[51] Pedras, M. H. J., and de Lemos, M. J. S., 2001, ''Adjustment of a Macroscopic Turbulence Model for a Porous Medium Formed by an Infinite Array of Elliptic Rods, *2nd International Conference on Computational Heat and Mass Transfer*, Rio de Janeiro, Brazil, October 22–26.
[52] Pedras, M. H. J., and de Lemos, M. J. S., 2001, ''Solução Numérica do Escoamento Turbulento num Meio Poroso Formado por Hastes Elípticas - Aplicação do Modelo k-ε Para baixo e Alto Reynolds,'' *Proc of COBEMOI - 16th Braz. Congr. Mech. Eng.*, (on CDROM) Uberlândia, MG, Brazil, November 26–30.